Practical Implications of Using the Ubiquitous Joint Models in Continuum Applications

Bijan Peik
Equilibrium Mining, Phoenix, USA

Andrew Tsai
Equilibrium Mining, Mississauga, Canada

Karl P. Lawrence
Equilibrium Mining, Phoenix, USA

Karen Moffitt
Equilibrium Mining, Brisbane, Australia

ABSTRACT: Failure mechanisms in open pit mining applications often involve a combination of weak rock mass and adverse structure. Major structure is typically included explicitly with less persistent fabric included using general anisotropy or ubiquitous joint constitutive models in both continuum and discontinuum applications. Implicit strength anisotropy in these constitutive models, however, is not equivalent to explicit jointed rock mass. This paper uses a conceptual slope example to illustrate that constitutive models incorporating ubiquitous joints exhibit an inherent strengthening which is considered a function of mesh density, mesh orientation, anisotropy orientation, and lateral constraint. The implication is an overestimate of the predicted stability margin by 5 – 10% or higher when key variables are compounded. Key observations are summarized with the intent to provide the reader with a guide to using ubiquitous joint models.

Keywords: Ubiquitous joint, Anisotropy, Numerical Modeling, Bedding, Slope Stability.

1 INTRODUCTION

Numerical simulation of anisotropic rock mass behavior has been the topic of rock engineering research for decades (Huang et al. 2022; Leng et al. 2021; Lu et al. 2020; Sainsbury et al. 2017). Unlike homogeneous engineered materials such as concrete, metal, plastic, etc., rock mass is a geologically formed heterogeneous and anisotropic material with a mechanical behavior controlled by a combination of intact rock mass properties and natural or induced directional weakness embedded through joints, bedding, foliation, and other discontinuities.

General anisotropy or ubiquitous joint (UJ) constitutive models allow for the implicit representation of discontinuities in continuum numerical models. Structural features are represented as preferential orientations of weakness in the rock mass as opposed to the explicit modeling of structure used in discontinuum models, which are limited in their applicability in large scale mining projects due to high computational costs. A detailed overview of UJ models can be found in Sainsbury et al. (2013).

UJ constitutive models are widely implemented in mining projects involving rock slopes, providing an efficient method of modelling anisotropic rock mass behavior in both two-dimensional

(2D) and three-dimensional (3D) applications (RocScience, 2023; Itasca, 2019). Many uncertainties remain however over its use in practical applications to inform design and operational decisions due to the common misconception that UJ models are indeed equivalent to discrete joints. Sainsbury et al. (2017) highlighted that UJ models do not consider the effects of joint spacing, length, stiffness, block interlocking, internal moments and bending rigidity of rock layers which results in misrepresentation of yielding and deformation response when compared to the more accurate discontinuum models. Carvalho et al. (2019) demonstrated that the implementation of UJ constitutive models can lead to unexpected stress and deformation behavior. Lu et al. (2020) demonstrated that the factor of safety is sensitive to the size of discretized mesh elements, until a certain threshold of element size is reached, and relatively insensitive to dilation and boundary extent.

In this paper, the response of the UJ model to mesh size, mesh alignment, UJ orientation, and lateral constraint were investigated with the goal of quantifying the uncertainty involved with using UJ models. The response is compared directly to analytical solutions to provide quantitative recommendations, with the primary objective of providing increased confidence in the use of UJ models and ultimately informing more reliable engineering decisions.

2 MOTIVATION

Major structural features (faults) are typically incorporated into continuum models through the use of discrete interfaces or embedded zones of (isotropically) weak rock mass. A simple slope model presented in Figure 1a was developed in FLAC3D (Itasca, 2019) to illustrate and verify the alternative approaches. Table 1 summarizes the default model configuration and assumed rock mass properties. Alternative mesh configurations were developed for demonstration purposes. A mesh aligned with the general orientation of the fault (min edge length 0.5 m) is displayed in Figure 1b, while Figure 1c displays a different configuration where the mesh is axis-aligned (i.e. octree mesh). When an octree mesh is used, the fault was modeled as a feature with 3-4 zone elements as previous studies indicate a minimum of 2-3 zones are required to resolve shear deformations correctly (Pierce et al., 2018). The fault was assumed cohesionless so that the analytical factor of safety (FOS) is known (FOS = tan(β)/tan(φ)).

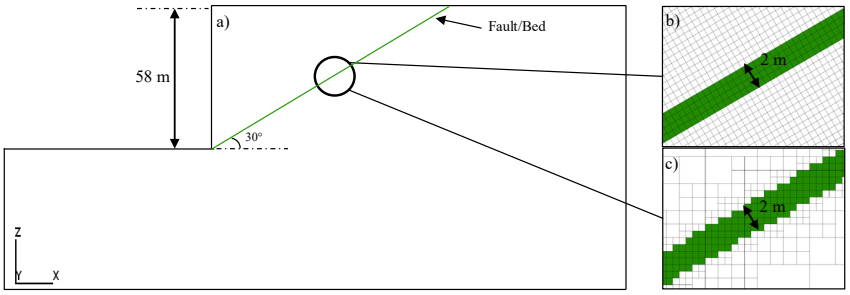

Figure 1. a) Slope example with fault orientated at 30° with inset of b) mesh aligned with the fault orientation and c) axis-aligned mesh, not aligned with the fault orientation.

Table 1. Default model configuration and rock mass properties.

Parameter	Description	Material Properties	Unit	Rock Mass	Fault
Slope Height	58 m	Density	[kg/m^3]	2000	2000
Fault Thickness	2 m (3-4 zone elements*)	Young Modulus	[GPa]	37	37
Fault Orientation, β	30°	Poisson Ratio	[-]	0.30	0.30
Mesh	0.5 m (min edge length)	Friction Angle, φ	[°]	60	30
		Cohesion, c	[MPa]	6	0
Boundary Conditions	Plane-strain (x-z), symmetry condition at lateral extents, fixed at base.	Dilation Angle, ψ	[°]	0	0

* A minimum of 3 zones is required when representing faults using weak zones to permit continuous shear.

The numerical model is used to estimate the strength reduction factor (SRF), analogous to FOS, using the Shear Strength Reduction (SSR) method. SRFs are estimated within a tolerance of 0.02, with the unstable SRF being reported in this paper. Stability margins are interpreted using results from incremental strength reductions instead of using internal commands (i.e., 'model factor-of-safety' command in FLAC3D) which should not be relied upon. Key variables that should be reviewed to inform stability are the unbalanced force, maximum mechanical ratio, yield states, deformation, velocities, and shear strain.

When the mesh is aligned with the fault, the estimated SRF for the interface, weak zone, and UJ models is approximately 1.0 as expected (Figure 1a). With an octree mesh (Figure 2b), the discrete and (isotropically) weak zone representations still predict an SRF = 1.0 – importantly, this highlights that faults can accurately be represented in numerical models using the weak zone approach and hexahedral / octree-based meshes (provided the thickness is represented by a minimum number of zones across the fault, which is maintained in the current study). When the (isotropically) weak zone is replaced with the UJ model (with anisotropy aligned with the fault orientation in an octree-based mesh), the estimated SRF increases to SRF = 1.08. Shearing through the host rock is prohibited in the UJ models by assigning increased strength to the rock mass. The only difference in this scenario (in comparison to the weak zone octree-based mesh or UJ fault-aligned mesh, both of which produce the analytical result of SRF = 1.0) is the orientation of the UJ relative to the octree mesh (and the restriction in direction of weakness).

This simple example highlights that there is an inherent, or at least numerically observed, strengthening of the fault when represented with the continuum based UJ constitutive models. This strengthening, together with the common misconception that UJ models represent discrete joints (interfaces), has been observed in many instances by the authors in application to rock slopes. It provides the motivation of the current study, which is to further assess and quantify, if possible, the dependency of the UJ strengthening on geometrical or numerical parameters that lead to this unexpected response.

3 SENSITIVITY ANALYSIS

Application of anisotropy for fault representation in numerical models is not common in practice. Many scenarios exist however, where foliated or heavily jointed geological units exist, at various thicknesses, between other units of significantly different strength. When UJ is used to represent discontinuities in these situations, strengthening can occur as demonstrated in the previous section. Sensitivities were considered in the following sub-sections to investigate the impact of varying parameters on estimated SRF. The term 'fault' is replaced with 'bed' in the analysis, so the reader is not biased towards considering the results are limited to fault representation.

3.1 Bed Thickness / Mesh Resolution

The default bed thickness is 2 m (with 0.5 m minimum edge length). A thicker 4 m and thinner beds of 1 m and 0.5 m were considered to assess the impact of bed thickness on the SRF. Note that the minimum mesh edge length was also varied at the same ratio to maintain a minimum of 3 - 4 zones across the thickness of the bed. The estimated SRF increases as the bed thickness decreases as illustrated in Figure 2. This indicates that the strengthening is amplified as the bed becomes thinner (and mesh becomes finer), which is counterintuitive as numerical results tend to be more accurate with increased mesh resolution.

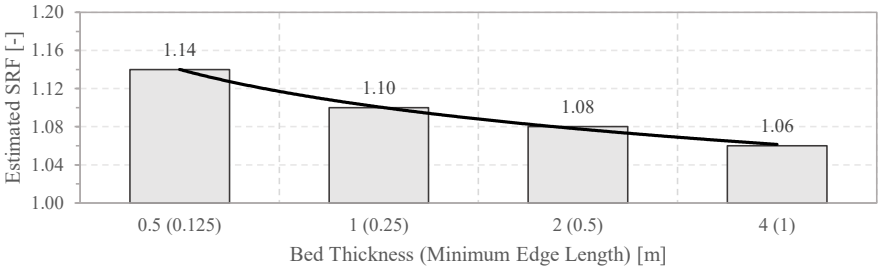

Figure 2. Estimated SRF for decreasing bed thickness.

In a second scenario, the thickness of the bed was held constant (2 m) while the mesh resolution was varied. The default minimum edge length for the bed is 0.5 m. A coarser resolution of 1 m and finer resolutions of 0.25 m and 0.125 m were considered to assess the impact of mesh resolution on the SRF. The estimated SRF decreases as the zone size (minimum edge length) decreases (Figure 3).

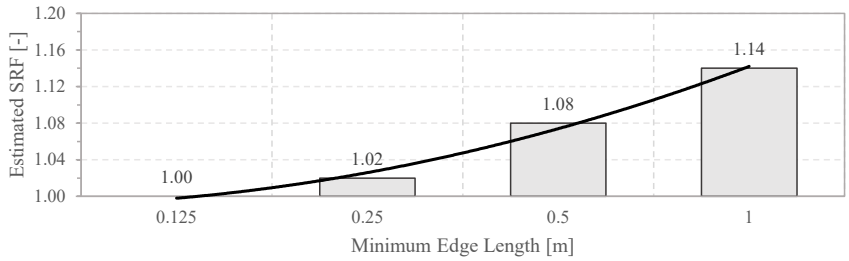

Figure 3. Estimated SRF for increasing mesh density (Constant bed thickness, 2m).

The models were independently confirmed to have an SRF = 1.0 when the weak zone approach was applied (to validate the mesh zone size is adequate to replicate the kinematic solution). The bed (Figure 2) thickness and mesh resolution (Figure 3) observations display opposite trends for decreasing edge length. The results are purposely presented in this manner to highlight the key conclusion: it is the lateral constraint on the UJ zones that enables the strengthening and not the mesh edge length/size or bed thickness considered individually. Note that the first column of both Figure 2 (SRF = 1.14) and Figure 3 (SRF = 1.00) have a mesh edge length of 0.125 m – but the bed is represented by (approximately) 4 elements in Figure 2, SRF = 1.14 (0.5 m bed thickness) and 16 elements in Figure 3, SRF = 1.00 (2 m bed thickness). As global stresses are limited by yield criteria in the UJ zones, this induces deformation and stress redistribution until numerical equilibrium is reached. The UJ stress correction is constrained within the thickness of the bed which prevents the failure mechanism from being fully transmitted through the bed. Figure 4 presents the yield state at SRF = 1.06 (Figure 4a) and SRF = 1.08 (Figure 4b) for the base scenario (minimum edge length of 0.5 m, and bed thickness of 2 m). This is one of the output variables reviewed in assessment of the SRF, but it is clear that at SRF = 1.06, a complete failure surface is not able to develop continuously along the full length of the bed (recall that it does develop at SRF = 1.0 if the weak zone approach is applied).

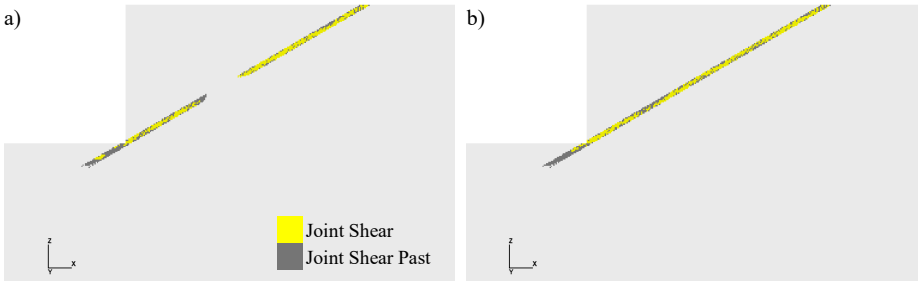

Figure 4. Yield state plots for a) SRF = 1.06 and b) SRF = 1.08.

3.2 *Lateral Constraint*

The results of Section 3.1 indicate a decreasing trend in SRF as the bed thickness is increased. This could be extrapolated to infer that at some bed thickness (> 4m, Figure 2) no strengthening will be observed. This was evaluated by increasing the upper lateral extent of the bed (until the entire slope contains the anisotropy) for the 30° orientation (Figure 5). The mesh resolution is fixed at the 0.5 m edge length. There is a decreasing trend as observed earlier, but the SRF does not reduce to 1.0 as expected. The model continues to over-predict the SRF by 4% when the entire slope is composed of a single homogeneous anisotropy.

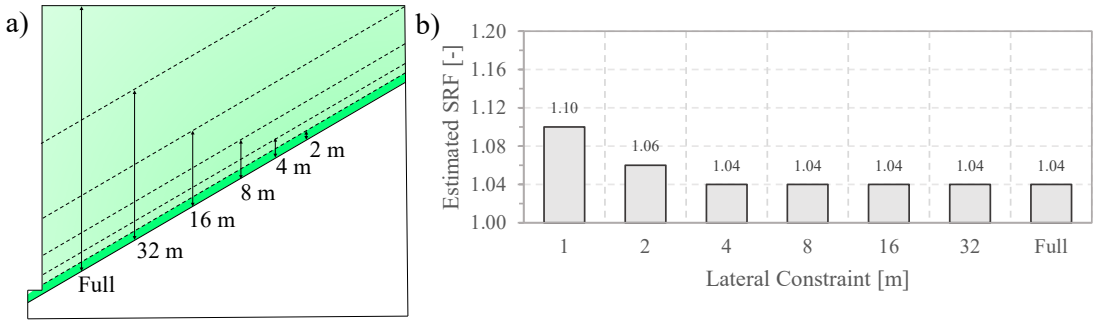

Figure 5. a) Schematic view of increasing bed thickness (lateral constraint) and b) Estimated SRF values for 100 kPa cohesion scenario.

3.3 *Bed Orientation*

The orientation of the anisotropy relative to the axis-aligned octree mesh was investigated by varying the dip of the bed from 20° to 70° by 5° increments (bed thickness fixed at 2 m). The anisotropy within the bed is always aligned parallel to the bed (Figure 6), scenario with and without cohesion is presented. The additional scenario was added as more prominent tensile failure is induced when the anisotropy / bed angle is increased beyond 45°, primarily due to the zero tensile strength (the UJ model has a tensile cutoff criterion which limits the upper bound on tensile strength to c/tan(φ) which is 0.0 in the cohesionless scenario). In the case with cohesion, the shear strength was adjusted by decreasing the friction angle, based upon the analytical solution, to achieve a target SRF = 1.0.

As the anisotropy orientation increases, the overprediction of SRF decreases as illustrated in Figure 6. Both cases display this trend, though the scenario with cohesion exhibits a slightly larger amount of strengthening. This lower SRF for the cohesionless scenario is also attributed to the tensile cutoff criteria at the lower angles. The increased component of vertical driving force, parallel to the overarching body forces (i.e., gravity), is hypothesized to be the reason for this trend. If this was purely anisotropy driven, the most adverse scenario would have been when the UJ orientation is aligned at 45° (as this produces the greatest angle between the underlying axis-aligned mesh and the UJ orientation). The key observation to note is that the amount of strengthening varies with UJ orientation (relative to the mesh alignment or body forces).

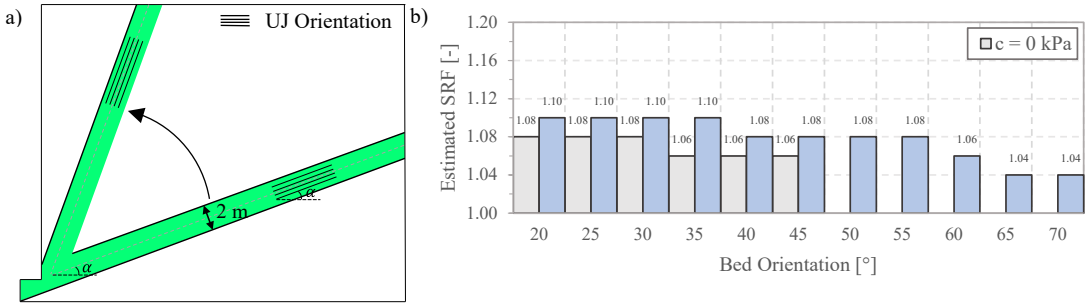

Figure 6. a) Schematic view of the increasing bed orientation (from 20° to 70°) with aligned anisotropy and b) Estimated SRF values for cohesionless and 100 kPa cohesion (Constant bed thickness, 2 m).

4 CONCLUSIONS AND RECOMMENDATIONS

A slope example was used to exhibit that anisotropy included implicitly in numerical models using UJ constitutive relationships experiences a strengthening phenomenon. This may have a significant impact on the predicted stability margins of large-scale mining operations, and therefore indirectly affect financial and risk-based decisions. Detailed interrogation of the analyses provides a lower bound estimate of 4-5% increase in shear strength. The amount of strengthening can increase substantially however, and be compounded by multiple factors, including the lateral constraint of the bed, the orientation of the anisotropy relative to the mesh (and body forces), and mesh density. This may lead to numerical models where the anisotropy in the UJ approach, though it is assumed infinitely intense and persistent, behaves 10-15% (or higher) stronger than discontinuity strengths obtained from laboratory testing. UJ constitutive models are considered accurately formulated and implemented in 3D stress modeling tools but should not be considered equivalent to the concept of discrete joints within a rock mass. Calibration of UJ models (as suggested by Sainsbury et al., 2018) is the most appropriate method to correlate the constitutive models to observed performance. However, this is not always possible due to the complexity of large-scale slope models, so the analysis presented herein attempts to provide an initial quantification of the bounds. Based upon the analyses presented in this paper, if proper back analyses to slope deformation or failure is not possible, a 5 – 10% decrease in UJ discontinuity strengths is recommended to simulate the intended response. This should be supplemented with local knowledge of rock mass conditions and additional numerical modeling (as suggested by other authors) as required, depending on the relative impact of the results and how much they contribute to decisions surrounding the financial, risk, and safety performance of a project.

REFERENCES

Carvalho, J. L., Lawrence, K. P., Moffitt, K., & Yetisir, M. 2019. Behaviour and realm of application of ubiquitous joint constitutive models – facts and limitations. *Proceedings of the 53rd US Rock Mechanics Symposium*, American Rock Mechanics Association.

Huang, J., Song, Y., Lei, M., Shi, C., Jia, C., & Zhang, J. 2022. Numerical simulation of anisotropic properties of shale under triaxial compression using 3D DEM. Research Square. DOI: 10.21203/rs.3.rs-2024410/v1

Itasca Consulting Group Inc. 2019. FLAC3D: Fast Lagrangian Analysis of Continua in Three-Dimensions, (Version 7.0), Minneapolis, United States.

Leng, X., Wang, C., Sheng, Q., Chen, J., & Li, H. 2021. An enhanced ubiquitous-joint model for a rock mass with conjugate joints and its application on excavation simulation of large underground caverns. *Frontiers in Earth Science*, 9. DOI: 10.3389/feart.2021.744900

Lu, R., Wei, W., Shang, K., & Jing, X. (2020). Stability analysis of jointed rock slope by strength reduction technique considering ubiquitous joint model. *Advances in Civil Engineering*. 2020. 1-13. DOI: 10.1155/2020/8862243

Pierce, M. & Garza-Cruz, T. (2018). *Answers to Questions Raised in March 16, 2018 Review of Itasca Analysis of Resolution Subsidence*. Itasca Consulting Group Inc. Technical Memorandum No. 2-4208-04:14TM15.

RocScience Inc. (2023). RS3 — 3D Finite Element Analysis Program.

Sainsbury, B.L. & Sainsbury, D.P. 2017. Practical use of the ubiquitous-joint constitutive model for the simulation of anisotropic rock masses. Rock Mechanics and Rock Engineering, 50, pp. 1507–1528.

Sainsbury, D.P. & Sainsbury, B.L. 2013. Three-dimensional analysis of pit slope stability in anisotropic rock masses. *Proceedings of the 2013 International Symposium on Slope Stability in Open Pit Mining and Civil Engineering*, Australian Centre for Geomechanics, Perth, pp. 683-695.